

SHARCS: HYBRID CONTROL CONCEPT FOR VIBRATION REDUCTION OF HELICOPTERS

Fatma Demet Ulker
fdulker@connect.carleton.ca

Andrei Mander
amander@connect.carleton.ca

Daniel Feszty
dfeszty@mae.carleton.ca

Fred Nitzsche
fnitzsch@mae.carleton.ca

Department of Mechanical and Aerospace Engineering, Carleton University
K1S5B6, Ottawa, ON, Canada

ABSTRACT

This paper summarizes the subsystem identification for the Smart Hybrid Active Rotor Control System (SHARCS). The SHARCS concept comprises of an Actively Controlled Flap and an Active Pitch Link operating simultaneously to reduce vibration and noise on helicopters. A scaled rotor is utilized as a demonstration platform for the hybrid control concept. This paper presents preliminary results of the system identification of the SHARCS blade, which were obtained both computationally from the SmartRotor aeroelastic code and experimentally from whirl tower tests, where the system characteristics at the nominal operational conditions were determined.

1. Introduction

Previous research has shown that actively controlled trailing edge flaps (TEFs) or active pitch links, when used individually, can successfully reduce vibration or noise on helicopter blades by changing the aerodynamic environment or the structural properties of the blade, respectively [1,2]. However, it has been observed that with only one system, optimum vibration and noise reduction cannot occur at the same, i.e. best vibration reduction occurred at different actuation than best noise reduction [1,2]. The novelty of the Smart Hybrid Active Control Rotor System (SHARCS) developed at Carleton University is that it employs multiple control systems to address simultaneous vibration and noise reduction. An added advantage of such system could also be the superior vibration reduction through simultaneous integration of multiple systems [3]. There are 3 systems proposed to be used on one single blade in the SHARCS project: the Active Pitch Link (APL), the Actively Controlled Flap (ACF) and the Actively Controlled Tip (ACT) (Figure 1). In this paper, preliminary results of vibration suppression performance for a dual component hybrid system (ACF and APL only) will only be presented.

Nowadays, the most popular active control system studied is the Trailing Edge Flap (TEF). Detailed investigations of vibration control using trailing edge flaps, carried out by Friedman and Chopra [4, 5], have led to full-scale rotors being built by Boeing Mesa and Eurocopter [6,1]. A major milestone was the first flight of a helicopter with an ACF by Eurocopter on a BK117

helicopter in the summer of 2005 [2]. Significant vibration reduction and noise reduction have been demonstrated in these tests.

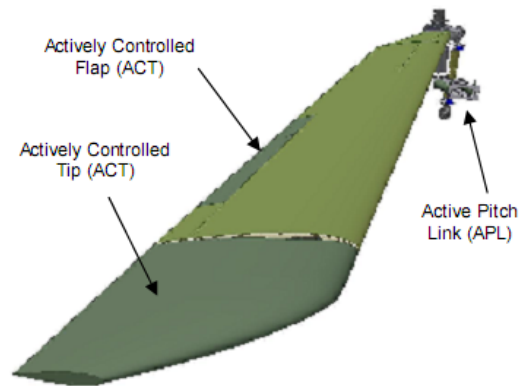


Figure 1: The SHARCS Concept With Three Individual Feedback Systems.

Another active control concept, the Active Pitch Link (APL) has also been considered by numerous researchers. For example, hydraulic based actuators were used by Eurocopter [7] and smart materials were demonstrated by Nitzsche et. al. [8-10].

The hybrid control approach proposed in the SHARCS project is based on the simultaneous control of both the structural and flow properties of the helicopter blade system. Structural control is achieved by the Active Pitch

Link (APL) which changes the structural properties of the blade resulting in a change in the blades modal frequencies, damping or both [10]. Flow control is achieved by the Actively Controlled Flap (ACF) which changes the effective camber of the helicopter blade via a trailing edge flap.

The purpose of the present paper is to provide preliminary results of the system identification of the control subsystems, both analytically and experimentally.

2. Aeroelastic model

A two-dimensional model of the aeroelastic system is illustrated in Figure 2. For control design purposes, the dynamics of both the APL and ACF mechanisms, including the helicopter rotor itself, must be modeled using input-output relationships. The APL and ACF mechanism models are identified using both analytical and open loop experimental methods. The open loop experiments were carried out in stationary (i.e. non-rotating) environment and in a whirl tower.

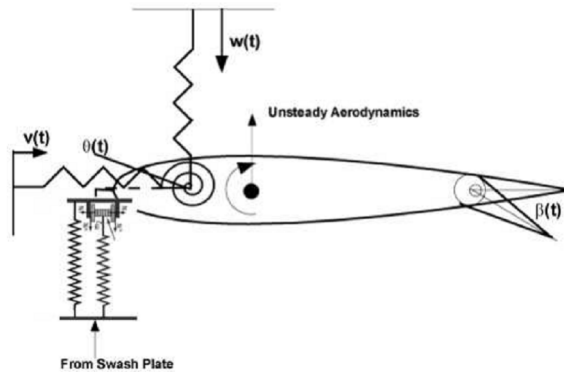


Figure 2: 2-D Representation of Aeroelastic Problem

System identification of the helicopter rotor was carried out using the SmartRotor aeroelastic solver. Within SmartRotor, the aerodynamic module consists on a Discrete Vortex Method developed at the National Technical University of Athens (NTUA) [11,12]. This consists of a panel method and vortex particle wake model allowing for flow field calculations around complex, multi-component configurations. A Finite Element Method structural module is used to model the structural response of the fully articulated helicopter blade. The APL is implemented as a sub-loop in the main aeroelastic calculation of SmartRotor which provides boundary condition for the pitch degree of freedom of the structural module.

In a forward flight regime, a helicopter behaves as Time Periodic (TP) system. For the purposes of controller design, several TP system identification techniques are available. Including, but not limited to, Periodic Auto Regressive Moving-Average (PARMA) [13], time lifting [14] and Harmonic Transfer Functions (HTF) [15-18], method. In this paper, the SHARCS blade rotating in forward flight is modeled using the HTF framework while the control subsystem models are developed from data gathered from whirl tower experiments.

3. System Identification Theory

As stated previously, for control purposes, it is necessary to identify input-output models of each of the control mechanism including the helicopter rotor itself. Due to the highly complex nature of the rotor blade's aeroelastic environment, its input-output characteristics are determined using system identification techniques. On the other hand, the input-output characteristics of the APL and ACF subsystems are obtained using both analytical and experimental results. Figure 3 illustrates the modeling approach used in this study.

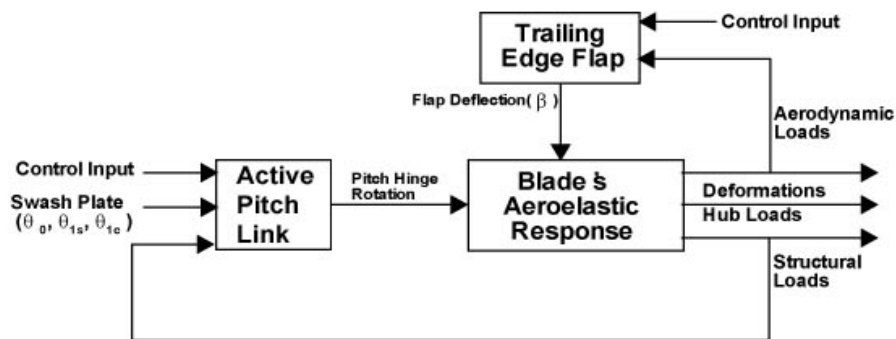


Figure 3: Block Diagram Representation of Helicopter Blade Control

4. System Identification – Computational Results

To demonstrate the capability of the SmartRotor code and the system identification approach, a typical forward flight condition featuring a rotational speed of $\Omega = 162.8$ rad/s and an advanced ratio of $\mu = 0.3$, was chosen. With a 3° shaft tilt, the swash plate collective and cyclic pitch were set as $\theta_0 = 5^\circ$, $\theta_{1c} = 1^\circ$, $\theta_{1s} = -1^\circ$, respectively.

Structural properties of the SHARCS blade, obtained from detailed finite element analysis, are introduced into to the SmartRotor code as an input file. Using the finite element code, a modal analysis of the SHARCS blade was performed. The first six eigen frequencies calculated at a rotational speed of $\Omega = 162.8$ rad/s were used to model the blade dynamics. Figure 4 shows the helicopter blade's wake as calculated using SmartRotor for the specified forward flight regime.

Mode	Frequency [1/rev]
1 st rigid lead-lag	0.23
1 st rigid flapping	1.03
1 st elastic beam bending	2.76
2 nd elastic beam bending	4.59
1 st elastic chord bending	4.29
1 st elastic torsion	6.03

Table 1: Eigen Frequencies of the SHARCS blade for a rotational speed of $\Omega=1628$ rad/s

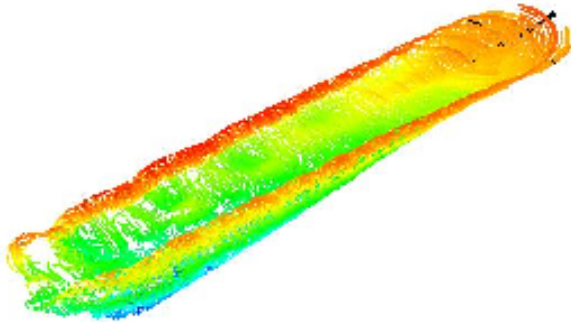
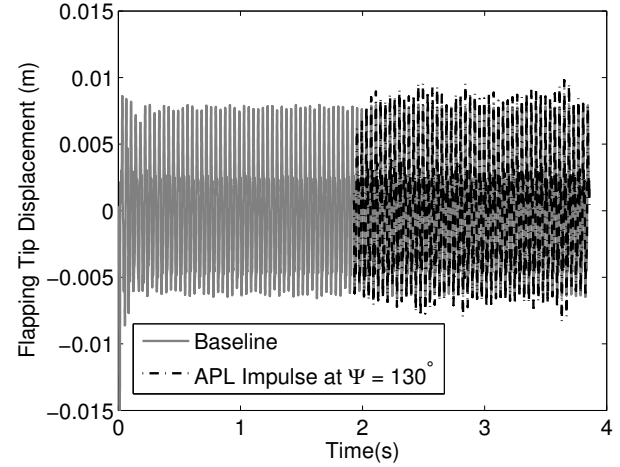


Figure 4: Wake of the SHARCS Blade in Forward Flight Baseline Case

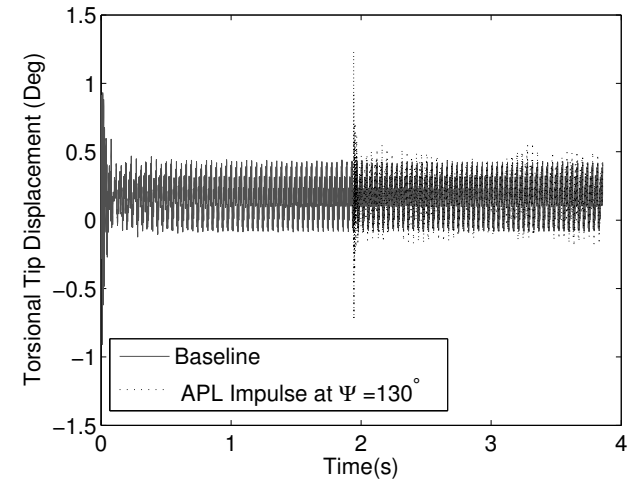
As illustrated in Figure 3, it is necessary to determine the input-output characteristics of the helicopter blade where the input comes from the APL and ACF. However, for the sake of brevity, we will limit our discussion to the effect of APL on the helicopter blade response. Therefore, the system identification problem is set as follows; determine the transfer function between APL and helicopter blade's response (deformations and/or hub

loads) under a particular flight regime and set pilot inputs.

In this paper, impulse responses are used to identify the rotor blade system. However, due to the time periodicity of the rotor blade environment, multiple impulses at varying azimuth angles must be applied. These responses can then be used to the synthesis of the Harmonic Transfer Function (HTF) model of the rotor blade.



(a) Flap-wise Direction



(b) Torsional-wise Direction

Figure 5 : Time Response of Tip Displacements Under the impulsive APL Displacement,
(Baseline : $\mu = 0.3$, $\theta_0 = 5$ deg, $\theta_{1c} = 1$ deg,
 $\theta_{1s} = -1$ deg, Tilt = 3 deg.)

In this preliminary analysis, each blade is considered to be independent of the others. However, it is obvious that in reality this is not true. The aerodynamic response

created by each blade will in turn affect each of the other blades on the rotor. In other words, a more detailed analysis would include identification of transfer functions that would model the effect of the blades on each other.

For illustration purposes, torsional and flap-wise tip deformation of the helicopter blade due to an impulsive displacement of APL at an azimuth angle of 130° are shown in Figure 5.

As expected, the impulse displacement of the APL has greatest influence in the blade torsional displacement response. As stated previously, the time periodic nature of the rotor blade in forward flight requires the application of impulses at varying azimuth angles. To illustrate this fact, Figure 6 shows the torsional tip displacement of the blade due to an impulsive displacement of APL applied at two different azimuth angles. Clearly, the two responses are not equal and therefore, the system must be time variant; specifically, time periodic.

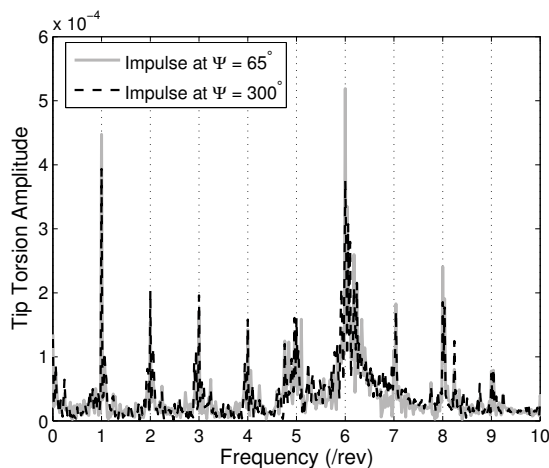


Figure 6: Frequency Response of Tip Torsional Displacements Under the impulsive APL Displacement Applied at Different Azimuth Angle (ψ)

Validation of the identified HTF model is necessary for completeness of the process. Figure 7 shows the force transmitted to pitch link obtained from the SmartRotor simulations and the System ID (SID) model due to sinusoidal APL displacement. Very good agreement was obtained.

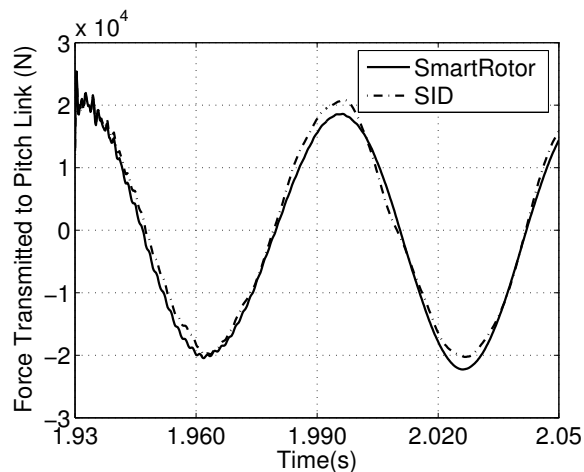


Figure 7: External Load Transmitted to the Pitch Link Resulting From Sinusoidal Excitation From APL

5. Active Pitch Link

The APL technology is based on utilizing the "Smart Spring" concept [20] which basic principle is shown in Figure 8. Here, spring k_1 represents the primary spring, whereas k_2 the secondary one. When the active material actuator is off, i.e. when mass m_2 can slide relative to the "Structure", it is only spring k_1 which translates the load to the "Structure". On the other hand, when the active material actuator is switched on, the friction force νN will be large enough to prevent m_2 from sliding and thus the system will have a stiffness of (k_1+k_2) , and both springs will contribute to translating the load to the structure.

In other words, a Smart Spring concept allows to change the stiffness of a system adaptively in the range of $k_1 \sim (k_1+k_2)$ by activating the smart material actuator. The main advantage of such configuration is that despite the small stroke, the large force of a piezoelectric actuator can be efficiently utilized.

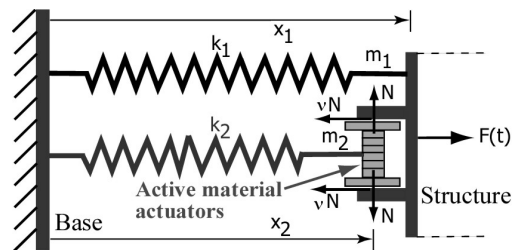


Figure 8: Schematic of the Smart Spring concept.

Results of the CFD simulations performed by SmartRotor are illustrated in Figures 9 and 10. As can be seen, the activation of the APL can efficiently reduce the vibration loads transmitted to the hub. More details on these studies are available in Refs. [8] and [21].

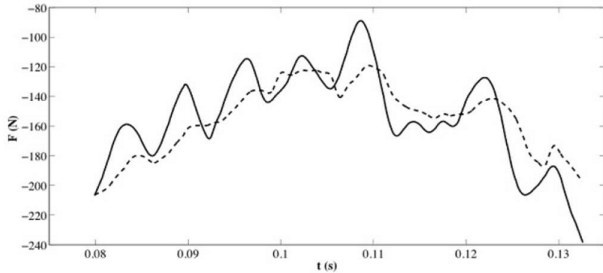


Figure 9: Transmitted loads during one blade revolution for the baseline (solid line) and active pitch link (dashed line) case. CFD simulation of forward flight at advance ratio of $\mu = 0.25$.

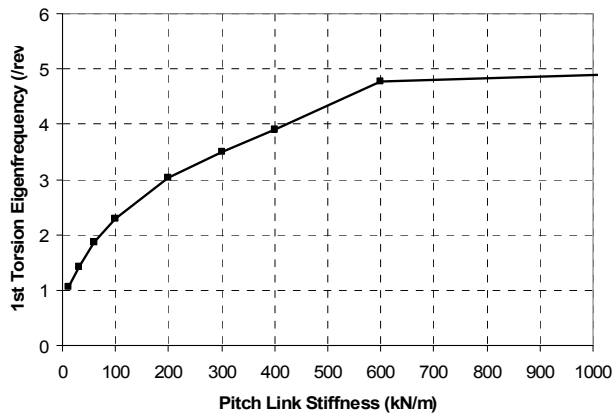


Figure 10: Effect of pitch link stiffness on the first elastic torsional modal frequency.

The APL Prototype is designed to continuously change its axial stiffness between 180 kN/m (“soft” mode) and infinity (“solid” mode).

To date, two versions of the APL have been built at Carleton University. A full-scale version was first developed to study the characteristics of the device in a non-rotating frame (Figure 11). Note that this design was dedicated purely for this particular test, the size and configuration of this model has not been optimized, only the functionality of the configuration was looked at. A full-scale helicopter blade was attached to the APL and vibratory loads were introduced via shakers.



Figure 11: Prototype of the full-scale model of APL

The second version was designed for conducting wind-tunnel tests in a 4 m x 4 m test section facility. It was optimized to be compact in size (120mm length) so that it can replace the conventional pitch link on the existing scaled rotor hub. The manufactured scaled prototype is shown in Figure 12.

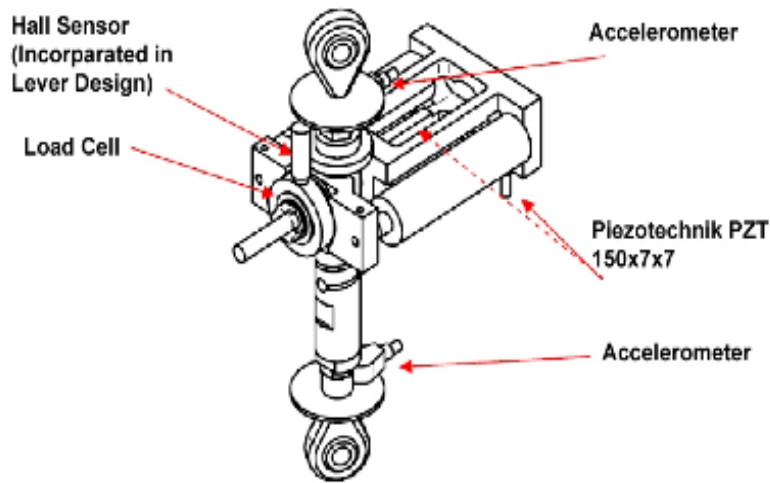


Figure 12: Prototype of the Acaled Active Pitch Link, Dedicated For Wind Tunnel Testing.

This APL features two modes, a “solid link” mode which has the stiffness of a conventional pitch link (practically infinity), and a “soft” mode, with controllable stiffness

values. The design is “fail-safe” i.e. if the piezoactuators fail, the “solid link” mode becomes functional. Operational modes are illustrated in Figure 13.

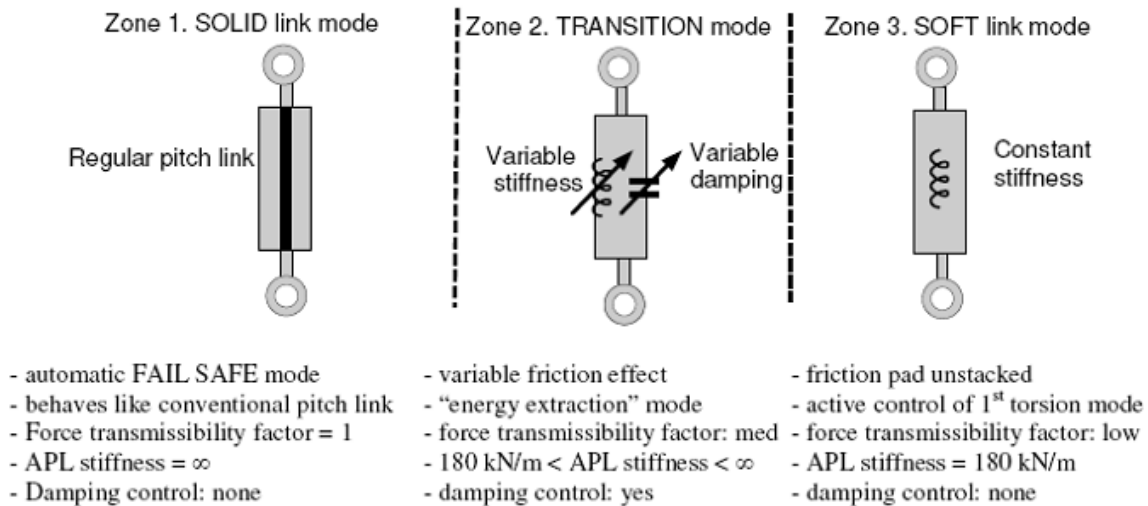


Figure 13: Theoretical Operational Modes of the Active Pitch Link

This prototype was first tested on a static test bench (Figure 14) which showed that the APL has wide control frequency range, acceptable linearity and high energy extraction factors. The experimental set-up was actively

tested with respect to the force transmissibility factor and blade modal shapes. The structural blade response was obtained using the LMS Modal Analysis toolbox and

compared to the frequency response function derived from CFD.

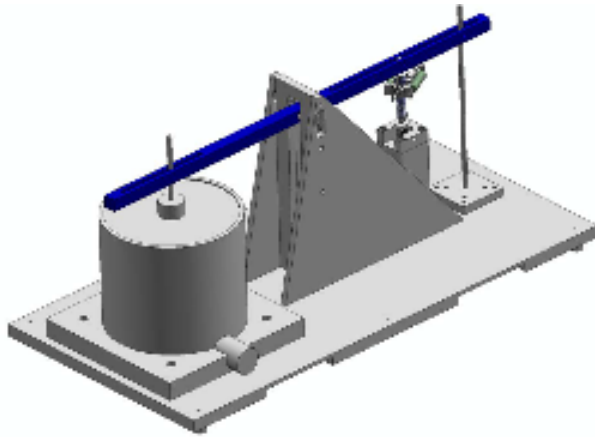


Figure 14: Static Test Jig for Testing the APL Prototype.

For the whirl tower tests, a special test jig has been developed since no vibrations can be reproduced in the lack of forward flight velocity component. This test jig is shown in Figure 16. It incorporated a large piezo-stack actuator to generate the typical vibratory loads experienced by the pitch link. The frequency and amplitude of these loads can be altered via the large piezo-stack actuators.

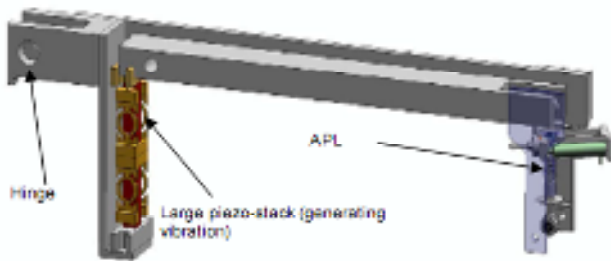


Figure 15: Whirl Tower Tests at DLR, Germany

The whirl tower tests (Figure 15) were completed at German Aerospace Agency DLR (Braunschweig, Germany). The performance of APL was tested under real centrifugal loads with rotational speeds up to 500rpm and applied normal force pitch link excitation in the frequency range up to 60 Hz. Experimental results were evaluated versus theoretical simulation results and static test data and illustrated in Figure 16.

The actual stiffness values on the Figure 16 were obtained as a relation of applied normal force from large piezo stack (see Figure 15) and actual displacement of APL obtained from Hall effect sensor data (see Figure 12). Experimental Dynamic test results have a good fit with Static results data in SOLID link and SOFT link zones. The performance of APL in TRANSITION zone was found limited due to the problems of friction sliding mechanism of APL under significant centrifugal loads. In order to use damping control strategy of APL in Transition zone some design improvements should be done.

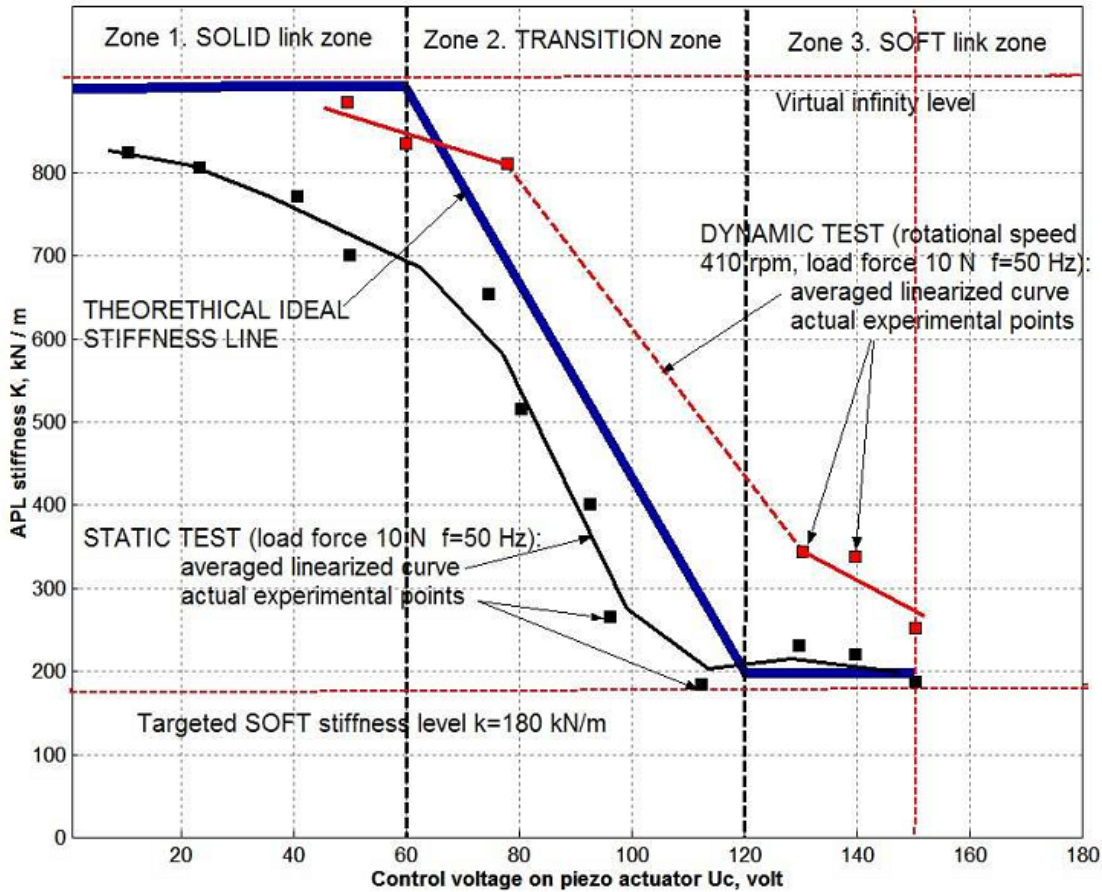


Figure 16: APL Stiffness Variation With Applied Voltage – Comparison of the Experimental Static (Black), Dynamic (Red) and Theoretical Results (Blue).

6. Actively Controlled Flap

The ACF actuator mechanism concept consists of a slider-cam mechanism shown in Figure 17, where the linear input displacement given by the piezoelectric

actuators is converted to an angular displacement of the flap. This is accomplished via a link system, which had to be optimized for the given actuator.

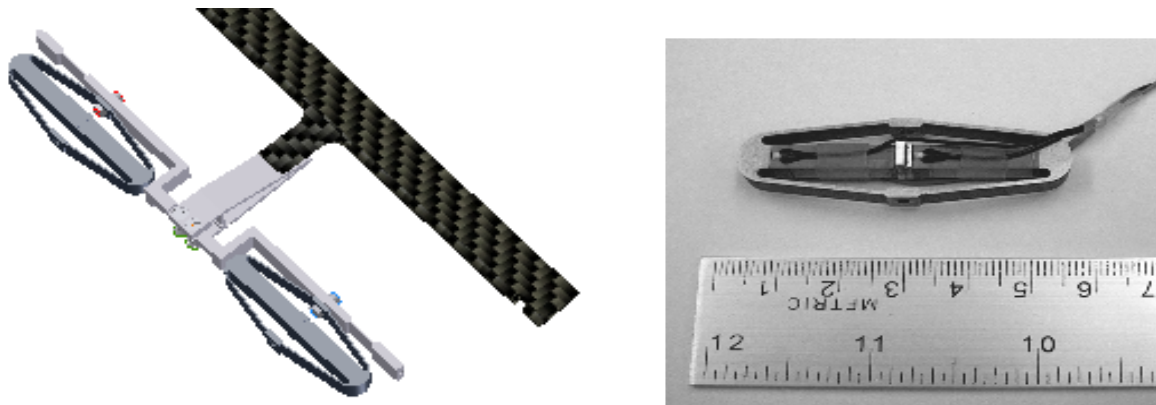
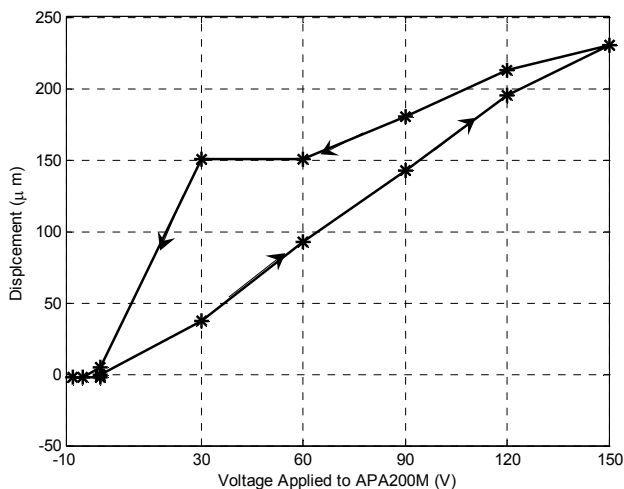


Figure 17 : The Concept of the ACF Flap Mechanism and the Selected Actuator

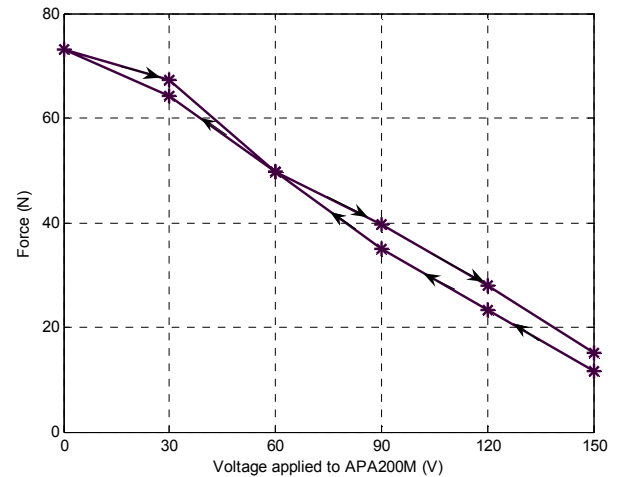
This mechanism was designed to provide 4 degrees downward flap deflection. Due to the relatively small size of SHARCS blade, it is not feasible to implement push-pull mechanism however, when upward-downward deflection pattern is required to be tested, the flap starting angle can be set to 2 degrees as the default.

Actuator selection is done considering the required moment to overcome the hinge moments due to both aerodynamic and inertial effects for the 4 degrees downward flap deflection. The hinge moment from aerodynamic loads was evaluated by using a 2D CFD analysis. The CMB (Carleton Multi Block) in-house RANS (Reynolds Averaged Navier-Stokes) solver [19] was used for the simulations. The flow conditions corresponded to those occurring at 75%R (midpoint of the flap) on the advancing blade in forward flight at $\mu = 0.3$ advance ratio. With the very conservative flow assumptions, steady simulations at 10 deg angle of attack (AOA) and 4 deg downward flap deflection were performed and aerodynamic hinge moments are obtained. Inertial loads are calculated for a mass 13.5gram of carbon fibre composite flap whose mass center located at $1/4^{\text{th}}$ of the flap chord. Considering the size requirements of SHARCS blade and the calculated required hinge moments, two APA 200M piezoelectric actuators shown in Figure 8 from Cedrat Ltd. were selected to be employed. Experiments are performed to determine their individual force and displacement characteristics under the applied voltage and presented in Figure 18.



(a) Displacement Change with Applied Voltage

The system was tested at rotational speeds of 400 to 1,550 RPM at 200 RPM increments. At each RPM increment, a sine sweep input signal was imposed to the actuators which drive the TE flap mechanism. Figure 11



(b) Force Change with Applied Voltage

Figure 18 : Hysteresis Behavior of APA200M

The experiments were performed in the non-rotating frame to define the properties and the capability of the mechanism. Then, the ACF design prototype was tested with a dummy flap at DLR Braunschweig’s whirl tower facility in November 2006 to verify the functionality of the mechanism under extreme centrifugal loads. A load cell was installed to monitor the actuation force, while accelerometers and a Hall effects sensor were used to monitor flap deflections. Figure 19 illustrates the whirl tower experimental setup.

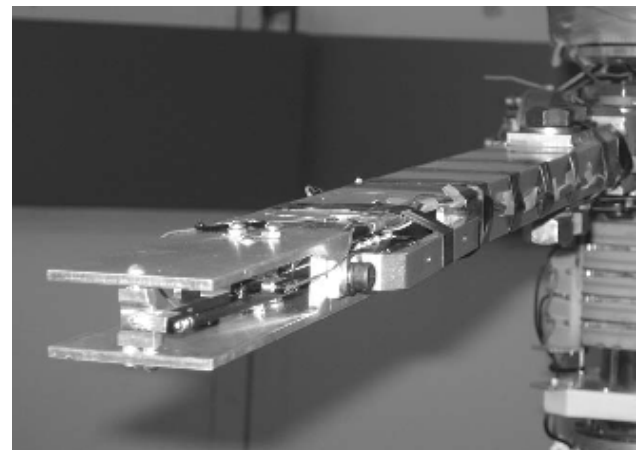


Figure 19: The ACF Installed at DLR Braunschweig’s Whirl Tower Facility

shows the frequency response of flap deflection measured by Hall Effect transducer at different rotational speed. However, after 1000 rpm it is observed that the obtained flap deflections are almost zero.

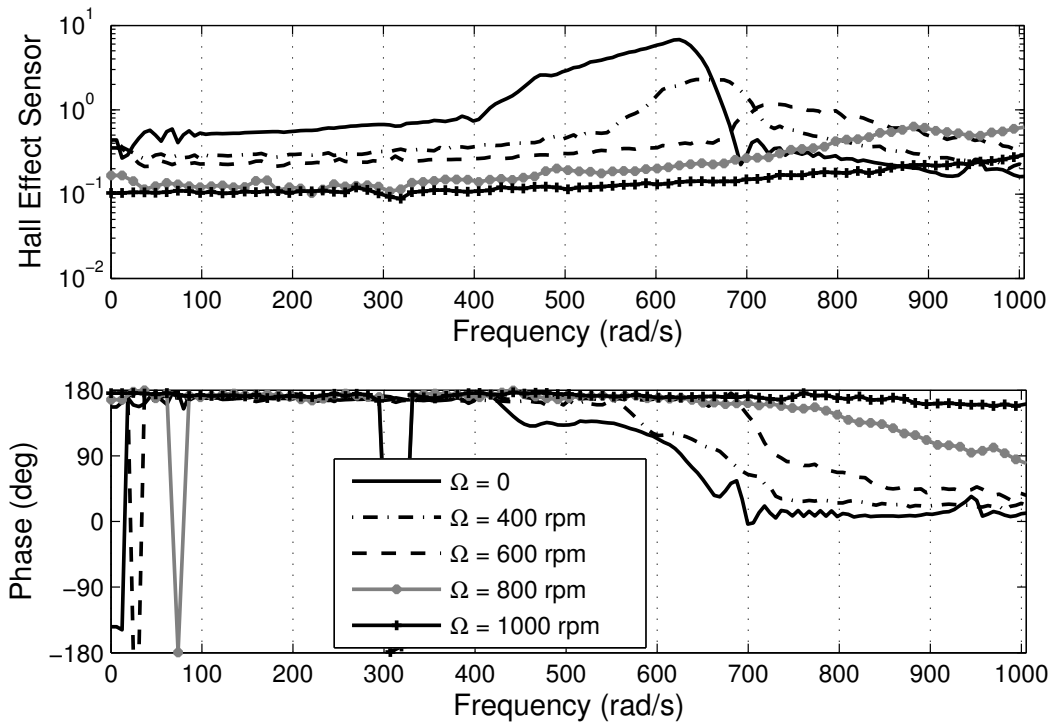


Figure 20: Frequency Response of the Flap Deflection Measured by Hall Effect Transducer

From the frequency response graph one can see the stiffening effect due to rotation. Another important observation is obtained from the change of DC gain of the Hall Effect transducer which is given in Figure 21. The DC gain of the Hall Effect transducer, which shows how flap is located with respect to blade (ie. Distance between Hall Effect transducer located on blade and the magnet located on flap) is decreasing with the rotational speed till 1000 rpm. We are aware that the mechanism could not function after 1000 rpm due to high centrifugal forces which brings to the conclusion of redesign of the ACF mechanism. However, under the centrifugal loading only, the ACF was able to produce 2 degrees of downward flap deflection up to 800 rpm.

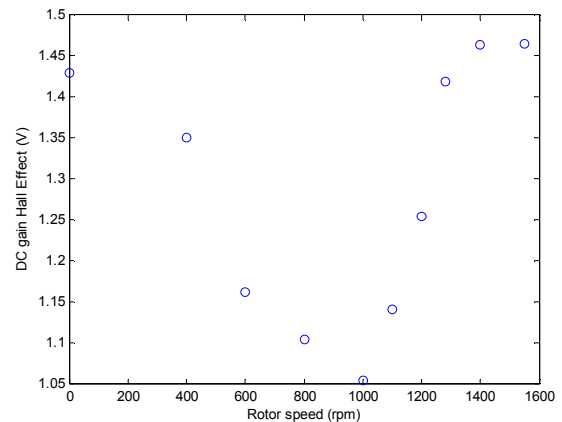


Figure 21 : Change in the DC volt of the Hall Effect Transducer with respect to RPM

For the proof of hybrid control concept, the ideal case is assumed where the designed mechanism has frequency response characteristic of that in the non-rotating case.

7. Conclusion

In this paper, brief review on the system identification of Smart Hybrid Active Rotor Control System was presented. Open loop system identification whirl tower experiments were performed for the determination of the system characteristics of the Actively Controlled Flap

and the Active Pitch Link systems at the operational conditions. It was concluded that further improvements are necessary before the wind tunnel experiments. Helicopter blade response was simulated using SmartRotor aeroelastic code and Harmonic Transfer Functions for the torsional tip deflections as well as vertical load transferred to the pitch link under the Active Pitch Link command. The comparison between the identified system output and SmartRotor simulations was presented.

References

1. Kloeppe, V., Enekl, B., Rotor Blade Control by Active Helicopter Servo Flaps”, International Forum on Aeroelasticity and Structural Dynamics (IFADS), Munich, Germany, paper no. IF-158, July 2005.
2. Roth, D., Enekl, B., Dietrich, O., Active rotor control by flaps for vibration reduction – full scale demonstrator and first flight test results, 32nd European Rotorcraft Forum, 12-14 Sep 2006, NLR, Maastricht, the Netherlands, Vol. 1, pp 801-814, 2007.
3. Feszty, D., Nitzsche, F., Khomutov, K., Lynch, B., Mander, A., Ülker, F.D., Design and instrumentation of the SHARCS scaled rotor with three independent control systems, Paper no. 080166, 64th Annual Forum of the American Helicopter Society, 29 April -1 May 2008, Montreal, QC, Canada, 2008.
4. Millott, T. A. and Friedmann, P. P., Vibration Reduction in Helicopter Rotors Using an Actively Controlled Partial Span Trailing Edge Flap Located on the Blade, NASA, CR4611, 1994.
5. Milgram, J., Chopra, I., Helicopter Vibration Reduction with Trailing Edge Flaps, 36th AIAA/ASME/ASCE/AHS/ASC Structures, Structural Dynamics and Materials Conference April 10-12 1995, New Orleans, LA.
6. Straub, F. K.; Kennedy, D. K.; Stemple, A. D.; Anand, V. R.; Birchette, T. S., Development and whirl tower test of the SMART active flap rotor, Smart Structures and Materials 2004 Industrial and Commercial Applications of Smart Structures Technologies. Edited by Anderson, Eric H. Proceedings of the SPIE, Volume 5388, p. 202-212, July 2004.
7. Jacklin, S.A., Blaas, A., Teves, D., Kube, R., Reduction of Helicopter BVI Noise, Vibration and Power Consumption through Individual Blade Control, 51st Annual Forum of the American Helicopter Society, Ft. Worth, Texas, 1995.
8. Nitzsche, F. and Oxley, G., Smart Spring Control of Vibration and Noise in Helicopter Blades, AIAA paper 2005-2270, presented at the 46th AIAA/ASME/ASCE/AHS/ASC Structures, Structural Dynamics and Materials Conference, Austin, Texas, Apr. 18-21, 2005.
9. A. Mander, D. Feszty, F. Nitzsche, Active Pitch Link Actuator for Impedance Control of Helicopter Vibration, The American Helicopter Society 64th Annual Forum, Montréal, Canada, April 29-May 1, 2008.
10. G.Coppotelli, P.Marzocca, F.D.Ulker, J.Campbell, and F.Nitzsche, Experimental Investigation on Modal Signature of Smart Spring/Helicopter Blade System, Journal of Aircraft, Vol.45,No.4, p: 1373-1380, July-August2008.
11. Voutsinas, S. G, Triantos, D. G., High-Resolution Aerodynamic Analysis of Full Helicopter Configurations, 25th European Rotorcraft Forum, Rome, Italy, Paper C11, 1999.
12. Vasilis A. Riziotis, Spyros G. Voutsinas. and Voutsinas, S. G., Aero-elastic Modeling Of The Active Flap Concept For Load Control, European Wind Energy Conference, 2008.
13. G. J. Adams, G. c. Goodwin, Parameter Estimation For Periodic ARMA Models, Journal of Time Series Analysis Vol. 16, No. 2, 1995.
14. Bittanti S., Colaneri, P, Invariant Representation of Discrete Time Periodic Systems, Automatica 36 p.1777-1793, 2000.
15. Wereley, M., N., Analysis and Control of Linear Periodically Time Varying Systems, PhD Thesis, Massachusetts Institute of Technology, February 1991.
16. Shin S., Integral Twist Actuation of Helicopter Rotor Blades For Vibration Reduction, PhD Thesis, Massachusetts Institute of Technology, August 2001.
17. Nitzsche,F., Laplace Domain approximation to the Transfer Functions of a Rotor Blade in Forward Flight, The Aeronautical Journal, pp233-240,May2001.
18. Siddiqi,A., Identification of the Harmonic Transfer Functions of a Helicopter Rotor, MSc Thesis, Massachusetts Institute of Technology, February 2001.
19. Davis, G.L., Feszty, D., Nitzsche, F., Trailing Edge Flow Control for the Mitigation of Dynamic Stall Effects, paper no. 053, 32nd European Rotorcraft Forum, Florence, Italy, Sep 2005.
20. Nitzsche, F., Zimcik, D., Wickramasinghe V, and Yong, C., Control laws for an active tunable vibration absorber designed for aeroelastic damping augmentation, The Aeronautical Journal, Vol. 108, No. 1079, 2004, pp. 35-42.
21. Nitzsche, F., Feszty, D., Waechter, D., Bianchi, E., Voutsinas, S., Gennaretti, M., Coppotelli, G., Ghiringhelli, G.L., The SHARCS Project: Smart Hybrid Active Rotor Control System for noise and vibration attenuation of helicopter rotor blades, paper No. 052, 31st European Rotorcraft Forum, Florence, Italy, September 2005.